Analytic Investigation and Numeric Prediction for Biodynamic Response of the Seated Human Body

Mostafa A. M. Abdeen[a], W. Abbas[b]

[a] Dept. of Eng. Mathematics and Physics, Faculty of Eng. Cairo University, Egypt
[b] Eng. Physics and Mathematics Dept., Faculty of Eng. (Mataria), Helwan University, Egypt
msotafa_a_m_abdeen@hotmail.com; wael_abass@hotmail.com

Abstract: The biodynamic response behaviors of seated human body subject to whole-body vibration have been widely investigated. The biodynamic response characteristics of seated human subjects have been extensively reported in terms of apparent mass and driving-point mechanical impedance while seat-to-head vibration transmissibility has been widely used to characterize response behavior of the seated subjects exposed to vibration. These functions (apparent mass, driving-point mechanical impedance) describe "to-the-body" force–motion relationship at the human–seat interface, while the transmissibility function describes "through-the-body" vibration transmission properties. The current study proposed a 4-DOF analytic biomechanical model of the human body in a sitting posture without backrest in vertical vibration direction to investigate the biodynamic responses of different masses and stiffness. Following the analytical approach, numerical technique developed in the present paper to facilitate and rapid the analysis. The numerical analysis used here applies one of the artificial intelligence technique to simulate and predict the response behaviors of seated human body for different masses and stiffness without the need to go through the analytic solution every time. The Artificial Neural Network (ANN) technique is introduced in the current study to predict the response behaviors for different masses and stiffness rather than those used in the analytic solution. The results of the numerical study showed that the ANN method with less effort was very efficiently capable of simulating and predicting the response behaviors of seated human body subject to whole-body vibration. [Journal of American Science. 2010;6(11):228-239]. (ISSN: 1545-1003).

Keywords: Biodynamic response, Analytic seated human body model, Numerical simulation model, Artificial Neural Network.

1. Introduction

The biodynamic responses of seated human occupant exposed to vibration have been widely characterized to define frequency-weightings for assessment of exposure, to identify human sensitivity and perception of vibration, and to develop seated body models [1]. The biodynamic response of the human body exposed to vibration have been invariably characterized through measurement of force motion relationship at the point of entry of vibration "To-the-body response function", expressed as the driving-point mechanical impedance (DPMI) or the apparent mass (APMS) and transmission of vibration to different body segments "Through-the-body response function", generally termed as seat-to-head transmissibility (STHT) for the seated occupant. Considering that the human body is a complex biological system, the "To-the-body" response function is conveniently characterized through non–invasive measurements at the driving point alone.

The vast majority of the reported studies on biodynamic response to whole-body vibration have considered vibration along the vertical axis alone. In many of the early studied, such as those conducted by

Coermann [2], Vogt [3], and Suggs [4], the numbers of subjects was usually relatively small, and only sinusoidal excitation was used, not generally representative of the type of excitation and levels of vibration usually encountered in practice. In many of these studies, the feet of the subjects were either not supported or supported but not vibrated, a condition not common in most driving situations. Fairley and Griffin [5], reported the vertical apparent mass of 60 seated subjects including men, women and children, which revealed a large scatter of data presumably owing to large variations in the subject masses. Boileau et al. [6] investigated the relationships between driving point mechanical impedance and seat-to-head transmissibility functions based upon 11 reported one dimensional lumped parameter models.

The majority of the models showed differences in frequencies corresponding to peak magnitudes of the two functions, which were expressed as resonant frequencies. Toward [7], summarized that a support of the back caused higher resonance frequency and slightly lower peak magnitude of the APMS response for subjects sitting on a horizontal plane. Wang et al. [8], study the

vertical apparent mass and seat-to-head transmissibility response characteristics of seated subjects are derived through measurements of total biodynamic force at the seat pan, and motions of the seat pan and head along the applied input acceleration direction, using 12 male subjects. The data were acquired under three different back support conditions and two different hands positions representative of drivers and passengers-like postures. Steina et al.[9], analyzed apparent mass measurements in the y- direction with a group of 13 male test subjects exposed to three excitation intensities.

In early studies, various biodynamic models have been developed to depict human motion from single-DOF to multi-DOF models. These models can be divided as distributed (finite element) models, lumped parameter models and multi-body models. The distributed model treats the spine as a layered structure of rigid elements, representing the vertebral bodies, and deformable elements representing the intervertebral discs by the finite element method. Multi-body human models are made of several rigid bodies interconnected by pin (two-dimensional) or ball and socket (three-dimensional) joints, and can be further separated into kinetic and kinematic models. It is clear that the lumped-parameter model is probably one of the most popular analytical methods in the study of biodynamic responses of seated human subjects, though it is limited to one-directional analysis. However, vertical vibration exposure of the driver is our main concern. Therefore, this paper carries out a thorough survey of literature on the lumped- parameter models for seated human subjects exposed to vertical vibration.

The lumped parameter models consider the human body as several rigid bodies and spring-dampers. This type of model is simple to analyze and easy to validate with experiments. However, the disadvantage is the limitation to one-directional analysis. Coermann [2], measured the driving-point impedance of the human body and suggested 1-DOF model. Suggs et al. [4], developed a 2-DOF human body. It was modeled as a damped spring-mass system to build a standardized vehicle seat testing procedure. A 3-DOF analytical model for a tractor seat suspension system is presented by Tewari et al. [10]. It was observed that the model could be employed as a tool in selection of optimal suspension parameters for any other type of vehicles. Boileau et al. [11] used an optimization procedure to establish a 4-DOF human model based on test data.

It is quite clear from the literature mentioned previously the amount of effort (experimentally or analytically) required to accurately investigate and understand the biodynamic response behaviors of

seated human body subject to whole-body vibration of different types and magnitudes. This fact urged the need for utilizing new technology and techniques to facilitate this comprehensive effort and at the same time preserving high accuracy.

Artificial intelligence has proven its capability in simulating and predicting the behavior of the different physical phenomena in most of the engineering fields. Artificial Neural Network (ANN) is one of the artificial intelligence techniques that have been incorporated in various scientific disciplines. Ramanitharan and Li [12] utilized ANN with back-propagation algorithm for modeling ocean curves that were presented by wave height and period. Abdeen [13] developed neural network model for predicting flow depths and average flow velocities along the channel reach when the geometrical properties of the channel cross sections were measured or vice versa. Allam [14] used the artificial intelligence technique to predict the effect of tunnel construction on nearby buildings which is the main factor in choosing the tunnel route. Allam, in her thesis, predicted the maximum and minimum differential settlement necessary precautionary measures. Azmathullah et al. [15] presented a study for estimating the scour characteristics downstream of a ski-jump bucket using Neural Networks (NN). Abdeen [16] presented a study for the development of ANN models to simulate flow behavior in open channel infested by submerged aquatic weeds. Mohamed [17] proposed an artificial neural network for the selection of optimal lateral load-resisting system for multi-story steel frames. Mohamed, in her master thesis, proposed the neural network to reduce the computing time consumed in the design iterations. Abdeen [18] utilized ANN technique for the development of various models to simulate the impacts of different submerged weeds' densities, different flow discharges, and different distributaries operation scheduling on the water surface profile in an experimental main open channel that supplies water to different distributaries.

2. Problem Description

To investigate the biodynamic response behaviors of seated human body subject to whole-body vibration (sinusoidal wave with amplitude 5 m/s^2), analytical and numerical techniques will be presented in this study. The analytical model and its results will be described in detail in the following sections. The numerical models presented in this study utilized Artificial Neural Network technique (ANN) using the data and the results of the analytical model to understand the biodynamic response behaviors and then can predict the behaviors for

different data of the human body without the need to go through the analytical solution.

3. Analytical Model
3.1 Biomechanical modeling

The human body in a sitting posture can be modeled as a mechanical system that is composed of several rigid bodies interconnected by springs and dampers. (Boileau and Rakheja [11]. This model as shown in Fig. 1 consists of four mass segments interconnected by four sets of springs and dampers. The four masses represent the following four body segments: the head and neck (m_1), the chest and upper torso (m_2), the lower torso (m_3), and the thighs and pelvis in contact with the seat (m_4). The mass due to lower legs and the feet is not included in this representation, assuming they have negligible contributions to the biodynamic response of the seated body. The stiffness and damping properties of thighs and pelvis are (k_4) and (c_4), the lower torso are (k_3) and (c_3), upper torsos are (k_2) and (c_2), and head are (k_1) and (c_1).

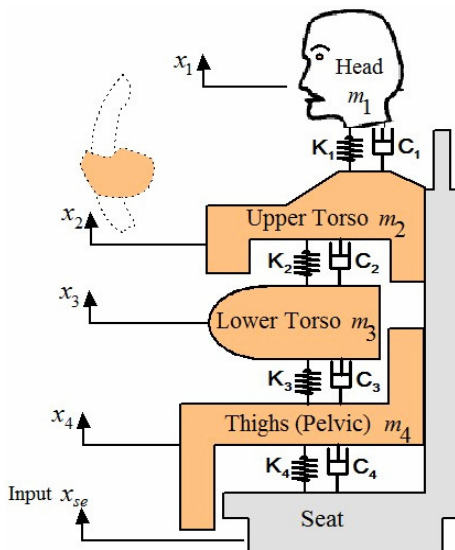The equation of motion of the human body can be obtained as follows:

Figure 1: Biomechanical Boileau and Rakheja 4-DOF model.

$$\begin{cases} m_1\ddot{x}_1 = -c_1(\dot{x}_1 - \dot{x}_2) - k_1(x_1 - x_2), \\[4pt] m_2\ddot{x}_2 = c_1(\dot{x}_1 - \dot{x}_2) + k_1(x_1 - x_2) \\ \qquad - c_2(\dot{x}_2 - \dot{x}_3) - k_2(x_2 - x_3) \\[4pt] m_3\ddot{x}_3 = c_2(\dot{x}_2 - \dot{x}_3) + k_2(x_2 - x_3) \\ \qquad - c_3(\dot{x}_3 - \dot{x}_4) - k_3(x_3 - x_4), \\[4pt] m_4\ddot{x}_4 = +c_3(\dot{x}_2 - \dot{x}_4) + k_3(x_2 - x_4) \\ \qquad - c_4(\dot{x}_4 - \dot{x}_{se}) - k_4(x_4 - x_{se}). \end{cases} \qquad (1)$$

The system equations of motion, equation (1), for the model can be expressed in matrix form as follows:

$$[M]\{\ddot{x}\} + [C]\{\dot{x}\} + [k]\{x\} = \{f\} \qquad (2)$$

Where $[M]$, $[C]$, and $[k]$ are $n \times n$ mass, damping, and stiffness matrices, respectively; $\{f\}$ is the force vector due to external excitation.

$$[M] = \begin{bmatrix} m_1 & 0 & 0 & 0 \\ 0 & m_2 & 0 & 0 \\ 0 & 0 & m_3 & 0 \\ 0 & 0 & 0 & m_4 \end{bmatrix},$$

$$[C] = \begin{bmatrix} c_1 & -c_1 & 0 & 0 \\ -c_1 & c_1 + c_2 & -c_2 & 0 \\ 0 & -c_2 & c_2 + c_3 & -c_3 \\ 0 & 0 & -c_3 & c_3 + c_4 \end{bmatrix},$$

$$[k] = \begin{bmatrix} k_1 & -k_1 & 0 & 0 \\ -k_1 & k_1 + k_2 & -k_2 & 0 \\ 0 & -k_2 & k_2 + k_3 & -k_3 \\ 0 & 0 & -k_3 & k_3 + k_4 \end{bmatrix},$$

And,

$$\{f\} = \begin{Bmatrix} 0 \\ 0 \\ 0 \\ c_4\dot{x}_{se} + k_4 x_{se} \end{Bmatrix}.$$

By taking the Fourier transformation of equation (2), the following matrix form of equation can be obtained:

$$\{X(j\omega)\} = [[K] - \omega^2[M] + j\omega[C]]^{-1} \{F(j\omega)\} \qquad (3)$$

Where, $\{X(j\omega)\}$ and $\{F(j\omega)\}$ are the complex Fourier transformation vectors of

$\{x\}$ and $\{f\}$, respectively. ω is the excitation frequency. Vector $\{X(j\omega)\}$ contains complex displacement responses of n mass segments as a function of ω ($\{X_1(j\omega), X_2(j\omega), X_3(j\omega), ..., X_n(j\omega)\}$). $\{F(j\omega)\}$ Consists of complex excitation forces on the mass segments as a function of ω as well.

3.2 Biodynamic response of human body

The biodynamic response of a seated human body exposed to whole-body vibration can be broadly categorized into two types. The first category "To-the-body" force motion interrelation as a function of frequency at the human-seat interface, expressed as the driving-point mechanical impedance (DPMI) or the apparent mass (APMS). The second category "Through-the-body" response function, generally termed as seat-to-head transmissibility (STHT) for the seated occupant.

The DPMI relates the driving force and resulting velocity response at the driving point (the seat-buttocks interface), and is given by [1]:

$$Z(j\omega) = \frac{F(j\omega)}{V(j\omega)} = \frac{F(j\omega)}{\dot{X}(j\omega)} \qquad (4)$$

Where, $Z(j\omega)$ is the complex DPMI, $F(j\omega)$ and $V(j\omega)$ or ($\dot{X}(j\omega)$) are the driving force and response velocity at the driving point, respectively. ω is the angular frequency in rad/s , and $j = \sqrt{-1}$ is the complex phasor.

Accordingly, DPMI for the model can be represented as:

$$DPMI(j\omega) = \left| \left(c_4 + \frac{k_4}{j\omega} \right) \frac{X_4(j\omega)}{X_0(\omega)} - \left(c_4 + \frac{k_4}{j\omega} \right) \right| \qquad (5)$$

In a similar manner, the apparent mass response relates the driving force to the resulting acceleration response, and is given by [19]:

$$APMS(j\omega) = \frac{F(j\omega)}{a(j\omega)} \qquad (6)$$

Where, $a(j\omega)$ is the acceleration response at the driving point

The magnitude of APMS offers a simple physical interpretation as it is equal to the static mass of the human body supported by the seat at very low frequencies, when the human body resembles that of a rigid mass. The above two functions are frequently used interchangeably, due to their direct relationship that given by:

$$APMS(j\omega) = \frac{DPMI(j\omega)}{j\omega} \qquad (7)$$

APMS for the model can be represented as:

$$APMS(j\omega) = \left| \frac{DPMI(j\omega)}{j\omega} \right| = \left| \left(\frac{c_4}{j\omega} + \frac{k_4}{-\omega^2} \right) \frac{X_4(j\omega)}{X_0(\omega)} - \left(\frac{c_4}{j\omega} + \frac{k_4}{-\omega^2} \right) \right| \qquad (8)$$

The biodynamic response characteristics of seated occupants exposed to whole body vibration can also be expressed in terms of seat-to-head transmissibility (STHT), which is termed as "through-the-body" response function. Unlike the force-motion relationship at the driving-point, the STHT function describes the transmission of vibration through the seated body. The STHT response function is expressed as:

$$H(j\omega) = \frac{a_H(j\omega)}{a(j\omega)} \qquad (9)$$

Where, $H(j\omega)$ is the complex STHT, $a_H(j\omega)$ is the response acceleration measured at the head of seated occupant, and $a(j\omega)$ is the acceleration response at the driving point. According to equation (9) seat-to-head transmissibility for the model is:

$$STHT(j\omega) = \frac{X_1(j\omega)}{X_0(\omega)} \qquad (10)$$

The above three functions have been widely used to characterize the biodynamic responses of the seated human subjects exposed to whole body vibration.

4. Analytic Results and Discussions

On the basis of anthropometric Boileau data [19], the proportion of total body weight estimated for different body segments is 7.5% for the head and neck, 40.2% for the chest and upper torso, 12.2% for the lower torso, and 18.2% for the thighs and upper legs. For a seated driver with mean body mass, maintaining an erect back not supported posture, 78% of the weight was found to be supported by the seat. The biomechanical parameters of the human model (Stiffness, Damping) are listed in Table 1.

Table 1: The biomechanical parameters of the Boileau and Rakheja model.

Stiffness Coefficient (N/m)	Damping coefficient (N.s/m)
$k_1 = 310000$	$c_1 = 400$
$k_2 = 183000$	$c_2 = 4750$
$k_3 = 162800$	$c_3 = 4585$
$k_4 = 90000$	$c_4 = 2064$

4.1 Response behaviors of the human body

In the following subsections the effect of body's mass, stiffness coefficient, and damping coefficient on the response behaviors of the human body (STHT, DPMI, and APMS) will be investigated using the analytical solution presented in the current study.

4.1.1 Effect of human body's mass

Three different total body masses (65, 75, and 85 kg) are used to investigate the effect of mass on the response behaviors of human body (STHT, DPMI and APMS) as shown in Fig. 2 (a, b, and c) respectively. From these figures, one can see that by

increasing the human body mass, the biodynamic response characteristics of seated human body (STHT, DPMI, and APMS) are increased.

4.1.2 Effect of stiffness coefficient

Three different values of pelvic stiffness k_4 (Boileau value (B.V.), B.V. +40%, and B.V. -40%) are used to investigate the effect of pelvic stiffness on the response behaviors of human body (STHT, DPMI and APMS) as shown in Fig. 3 (a, b, and c) respectively. From these figures, it is clear that by increasing the pelvic stiffness, the biodynamic response characteristics of seated human body (STHT, DPMI, and APMS) are increased.
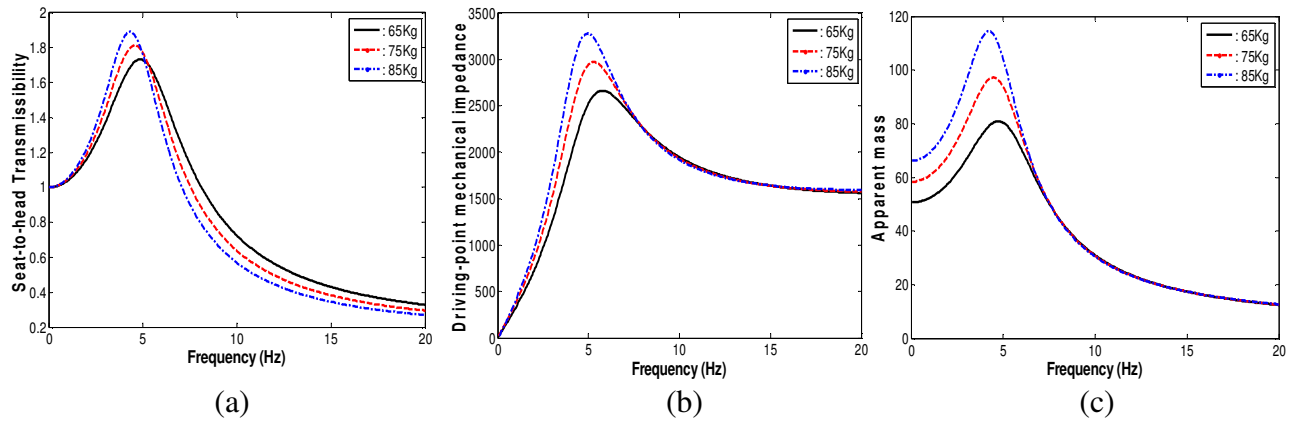

(a)   (b)   (c)

Figure 2: Effect of human body's mass on the biodynamic response behaviors (Analytic Results) ((a)STHT, (b) DPMI and (c) APMS)

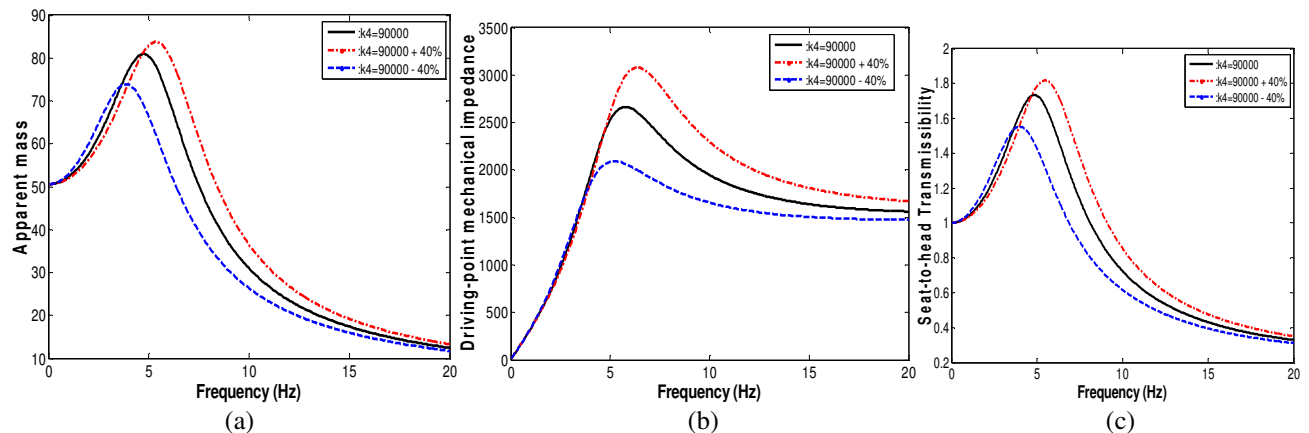(a)   (b)   (c)

Figure 3: Effect of stiffness coefficient on the biodynamic response behaviors (Analytic Results) ((a) STHT, (b) DPMI and (c) APMS)
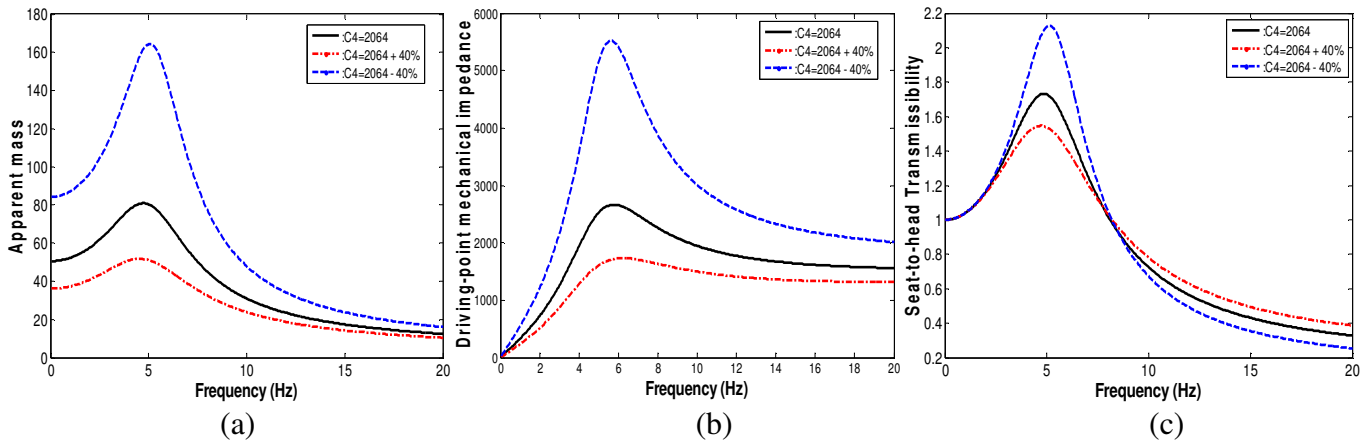
Figure 4: Effect of damping coefficient on the biodynamic response behaviors (Analytic Results)
((a) STHT, (b) DPMI and (c) APMS)

4.1.3 Effect of damping coefficient

Three different values of pelvic damping coefficient C_4 (Boileau value (B.V.), B.V. +40%, and B.V. -40%) are used to investigate the effect of pelvic damping coefficient on the response behaviors of human body (STHT, DPMI and APMS) as shown in Fig. 4 (a, b, and c) respectively. From these figures, it is clear that by increasing pelvic damping coefficient, the biodynamic response characteristics of seated human body (STHT, DPMI, and APMS) are decreased.

5. Numerical Model Structure

Neural networks are models of biological neural structures. Abdeen [13] described in a very detailed fashion the structure of any neural network. Briefly, the starting point for most networks is a model neuron as shown in Fig. 5. This neuron is connected to multiple inputs and produces a single output. Each input is modified by a weighting value (w). The neuron will combine these weighted inputs with reference to a threshold value and an activation function, will determine its output. This behavior follows closely the real neurons work of the human's brain. In the network structure, the input layer is considered a distributor of the signals from the external world while hidden layers are considered to be feature detectors of such signals. On the other hand, the output layer is considered as a collector of the features detected and the producer of the response.
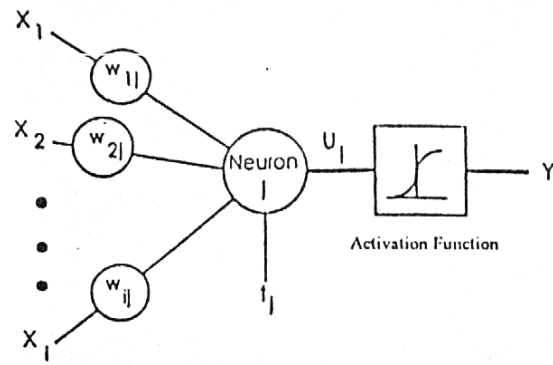

Figure 5: Typical picture of a model neuron that exists in every neural network

5.1 Neural Network Operation

It is quite important for the reader to understand how the neural network operates to simulate different physical problems. The output of each neuron is a function of its inputs (X_i). In more details, the output (Y_j) of the jth neuron in any layer is described by two sets of equations as follows:

$$U_j = \Sigma \left(X_i w_{ij} \right) \tag{11}$$

And

$$Y_j = F_{th} \left(U_j + t_j \right) \tag{12}$$

For every neuron, j, in a layer, each of the i inputs, X_i, to that layer is multiplied by a previously established weight, w_{ij}. These are all summed together, resulting in the internal value of this operation, U_j. This value is then biased by a

previously established threshold value, t_j, and sent through an activation function, F_{th}. This activation function can take several forms such as Step, Linear, Sigmoid, Hyperbolic, and Gaussian functions. The Hyperbolic function, used in this study, is shaped exactly as the Sigmoid one with the same mathematical representation, as in equation (13), but it ranges from -1 to $+1$ rather than from 0 to 1 as in the Sigmoid one (Fig. 6)

$$f(x) = \frac{1}{1 + e^{-x}} \qquad (13)$$

The resulting output, Y_j, is an input to the next layer or it is a response of the neural network if it is the last layer. In applying the Neural Network technique, in this study, Neuralyst Software, Shin [20], was used.
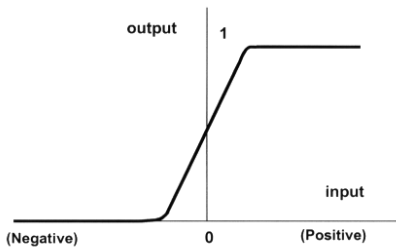

Figure 6: The Sigmoid Activation Function

5.2 Neural Network Training

The next step in neural network procedure is the training operation. The main purpose of this operation is to tune up the network to what it should produce as a response. From the difference between the desired response and the actual response, the error is determined and a portion of it is back propagated through the network. At each neuron in the network, the error is used to adjust the weights and the threshold value of this neuron. Consequently, the error in the network will be less for the same inputs at the next iteration. This corrective procedure is applied continuously and repetitively for each set of inputs and corresponding set of outputs. This procedure will decrease the individual or total error in the responses to reach a desired tolerance.

Once the network reduces the total error to the satisfactory limit, the training process may stop. The error propagation in the network starts at the output layer with the following equations:

$$w_{ij} = w'_{ij} + LR(e_j X_i) \qquad (14)$$

And,

$$e_j = Y_j (1 - Y_j)(d_j - Y_j) \qquad (15)$$

Where, w_{ij} is the corrected weight, w'_{ij} is the previous weight value, LR is the learning rate, e_j is the error term, X_i is the ith input value, Y_j is the output, and d_j is the desired output.

6. Numerical Simulation Cases

To fully investigate numerically the biodynamic response behaviors of seated human body subject to whole body vibration, several simulation cases are considered in this study. These simulation cases can be divided into two groups to simulate the response behaviors due to changing of human body's mass and stiffness respectively. From the analytic investigation, it is clear that the effect of damping coefficient is opposite to the effect of stiffness coefficient on the response behaviors of the human body. So in the numerical analysis, the effect of stiffness coefficient will be studied only in addition with the effect of human body's mass.

6.1 Neural Network Design

To develop a neural network model to simulate the effect of mass and stiffness on the biodynamic response behaviors of seated human body, first input and output variables have to be determined. Input variables are chosen according to the nature of the problem and the type of data that would be collected. To clearly specify the key input variables for each neural network simulation group and their associated outputs, Tables 2 and 3 are designed to summarize all neural network key input and output variables for the first and second simulation groups respectively.

It can be noticed from Tables 2 and 3 that every simulation group consists of three simulation cases (three neural network models) to study the effect of mass and stiffness on the seat-to-head transmissibility (STHT), driving point mechanical impedance (DPMI) and apparent mass (APMS).

Table 2: Key input and output variables for the first neural network simulation group (effect of human body's mass)

Simulation Case	Input Variables					Output
STHT	m_1	m_2	m_3	m_4	Frequency	STHT
DPMI						DPMI
APMS						APMS

Table 3: Key input and output variables for the second neural network simulation group (effect of stiffness coefficient)

Simulation Case	Input Variables		Output
STHT			STHT
DPMI	k_4	Frequency	DPMI
APMS			APMS

Several neural network architectures are designed and tested for all simulation cases investigated in this study to finally determine the best network models to simulate, very accurately, the effect of mass and stiffness based on minimizing the

Root Mean Square Error (RMS-Error). Fig. 7 shows a schematic diagram for a generic neural network. The training procedure for the developed ANN models, in the current study, uses the data from the results of the analytical model to let the ANN understands the behaviors. After sitting finally the ANN models, these models are used to predict the biodynamic response behaviors for different masses and stiffness rather than those used in the analytic solution.

Table 4 shows the final neural network models for the two simulation groups and their associate number of neurons. The input and output layers represent the key input and output variables described previously for each simulation group.
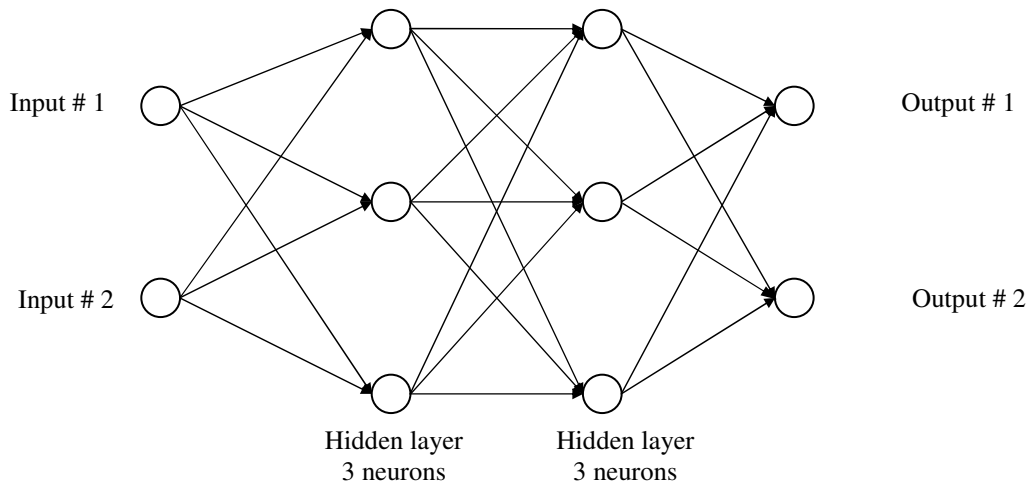

Figure 7: General schematic diagram of asimple generic neural network

Table 4: The developed neural network models for all the simulation cases

Simulation Group		No. of Layers	No. of Neurons in each Layer				
			Input Layer	First Hidden	Second Hidden	Third Hidden	Output Layer
First Group (mass)	STHT	5	5	6	4	2	1
	DPMI	4	5	6	4	-	1
	APMS						
Second Group (Stiffness)	STHT	4	2	5	3	-	1
	DPMI						
	APMS						

Table 5: Parameters used in the developed neural network models

Simulation Group		Training Epochs	MPRE	RMS-Error
First Group (mass)	STHT	45931	1.213	0.0015
	DPMI	7560	2.609	0.0022
	APMS	7174	3.743	0.0023
Second Group (Stiffness)	STHT	14012	3.449	0.0014
	DPMI	100185	3.938	0.002
	APMS	101463	1.644	0.0012

The parameters of the various network models developed in the current study for the different simulation models are presented in table 5. These parameters can be described with their tasks as follows:

Learning Rate (LR): determines the magnitude of the correction term applied to adjust each neuron's weights during training process = 1 in the current study.

Momentum (M): determines the "life time" of a correction term as the training process takes place = 0.9 in the current study.

Training Tolerance (TRT): defines the percentage error allowed in comparing the neural network output to the target value to be scored as "Right" during the training process = 0.001 in the current study.

Testing Tolerance (TST): it is similar to Training Tolerance, but it is applied to the neural network outputs and the target values only for the test data = 0.003 in the current study.

Input Noise (IN): provides a slight random variation to each input value for every training epoch = 0 in the current study.

Function Gain (FG): allows a change in the scaling or width of the selected function = 1 in the current study.

Scaling Margin (SM): adds additional headroom, as a percentage of range, to the rescaling computations used by Neuralyst Software, Shin (1994), in preparing data for the neural network or interpreting data from the neural network = 0.1 in the current study.

Training Epochs: number of trails to achieve the present accuracy.

Percentage Relative Error (PRR): percentage relative error between the numerical results and actual measured value and is computed according to equation (16) as follows:

PRE = (Absolute Value (ANN_PR - AMV)/AMV)*100   (16)

Where:

ANN_PR: Predicted results using the developed ANN model

AMV   : Actual Measured Value

MPRE: Maximum percentage relative error during the model results for the training step.

7. Numeric Results and Discussions

Numerical results using ANN technique will be presented in this section for the two groups (six models) to show the simulation and prediction powers of ANN technique for the effect of human body's mass and stiffness coefficient on the biodynamic response behaviors (STHT, DPMI and APMS) subject to whole-body vibration.

7.1 Effect of human body's mass

Three ANN models are developed to simulate and predict the effect of human body's mass on the biodynamic response behaviors (STHT, DPMI and APMS). Figures 8, 9, and 10 show the ANN results and analytical ones for different human body's masses. From ANN training figures (Left), it is very clear that ANN understands and simulates very well the biodynamic response behaviors. After that the developed ANN models used very successfully and efficiently to predict the response behaviors for different masses rather than those used in the analytic solution as shown in the predicted figures of ANN results (Right).

### 7.2 Effect of stiffness coefficient

Another three ANN models are developed in this sub-section to simulate and predict the effect of stiffness coefficient (k_4) on the biodynamic response behaviors (STHT, DPMI and APMS). Figures 11, 12, and 13 show the ANN results and analytical ones for different values of k_4. From ANN training figures (Left), it is very clear that ANN understands and simulates very well the biodynamic response behaviors. After that the developed ANN models used very successfully and efficiently to predict the response behaviors for different values of k_4 rather than those used in the analytic solution as shown in the predicted figures of ANN results(Right).
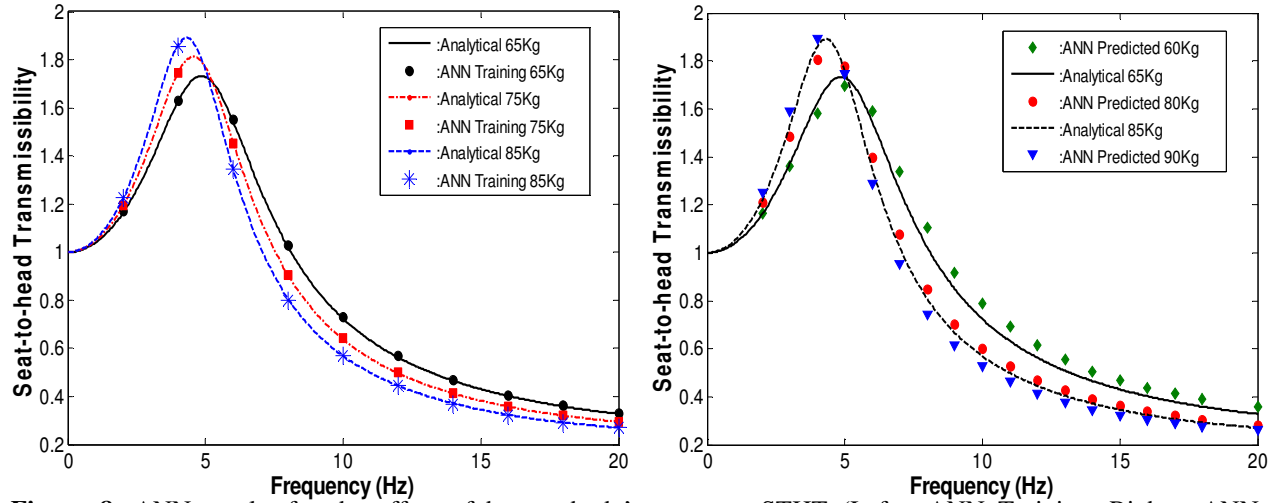
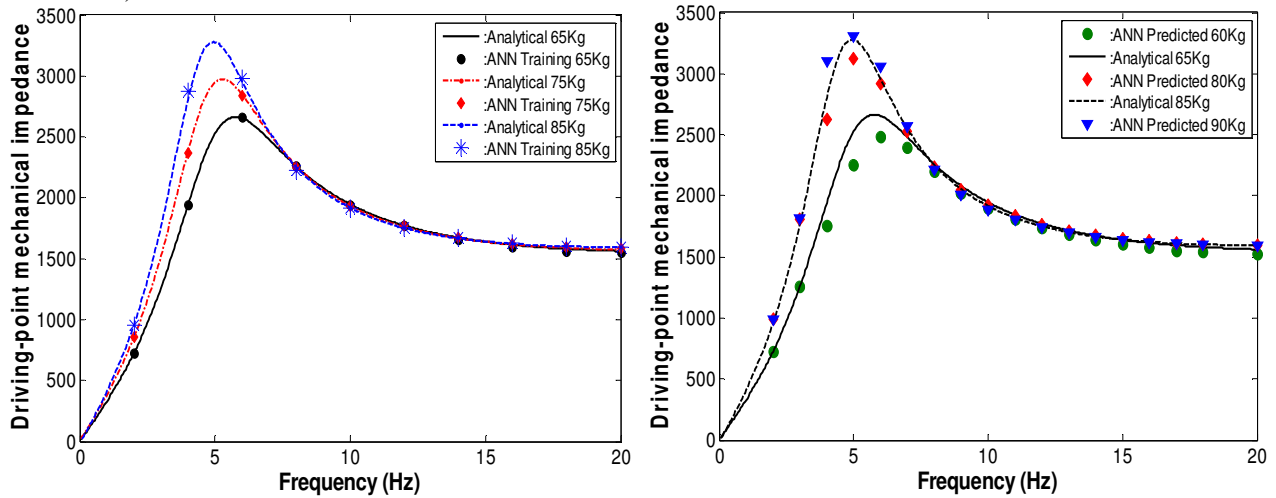**Figure 8**: ANN results for the effect of human body's mass on STHT (Left : ANN Training, Right : ANN Prediction)

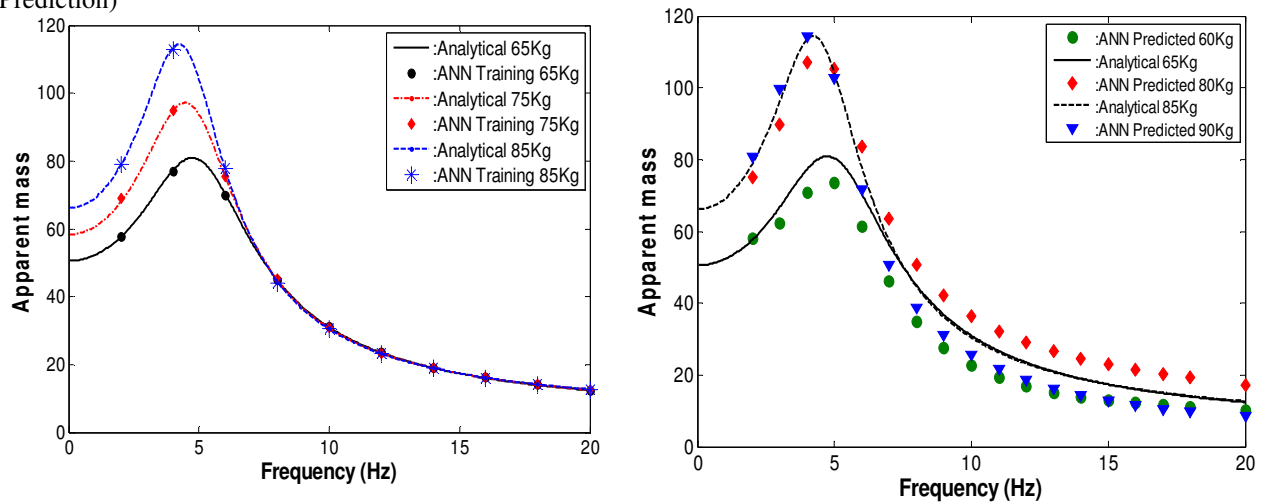**Figure 9:** ANN results for the effect of human body's mass on DPMI(Left : ANN Training, Right : ANN Prediction)

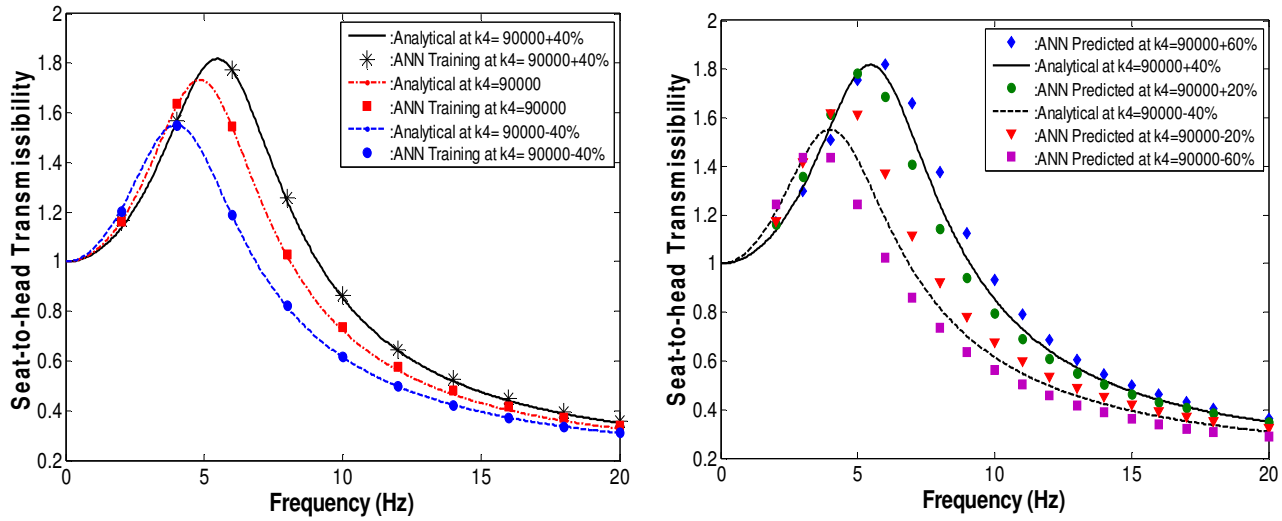**Figure 10:** ANN results for the effect of human body's mass on APMS(Left : ANN Training, Right : ANN Prediction)

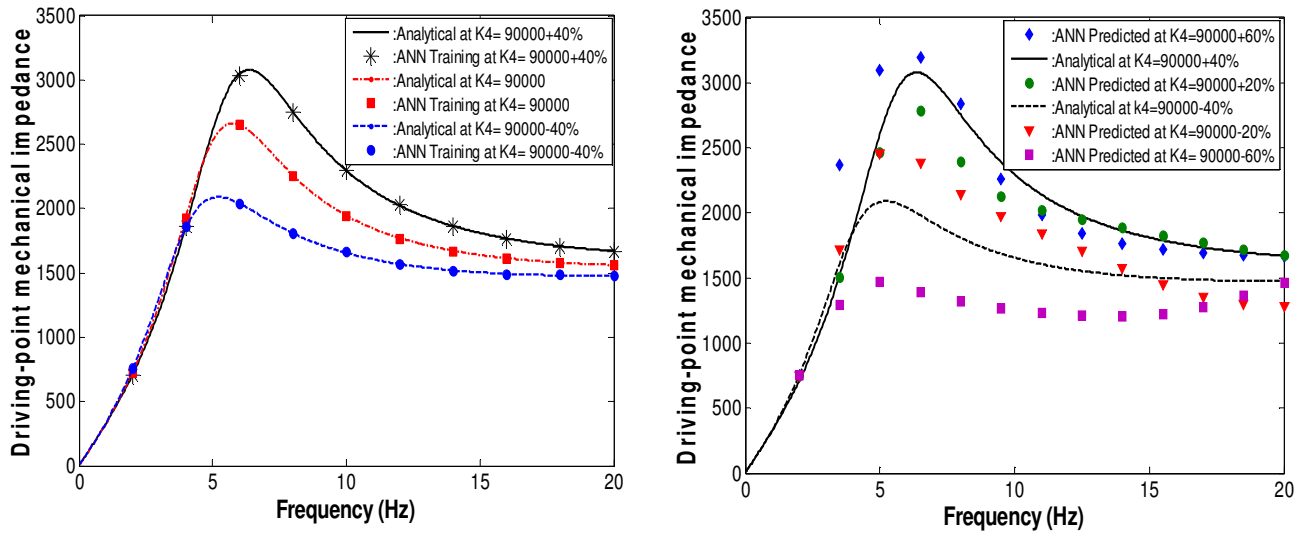**Figure 11**: ANN results for the effect stiffness coefficient on STHT(Left : ANN Training, Right : ANN Prediction)

Figure 12: ANN results for the effect stiffness coefficient on DPMI(Left : ANN Training, Right : ANN Prediction)
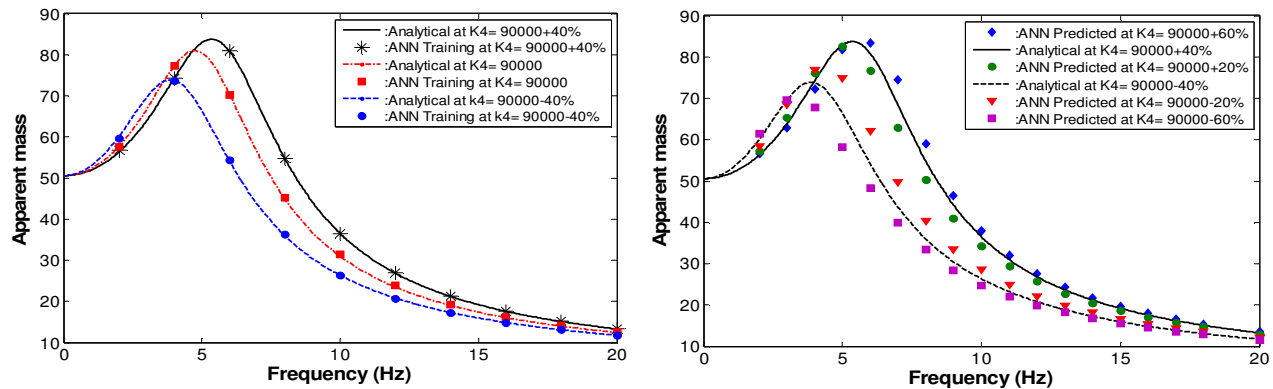

Figure 13: ANN results for the effect stiffness coefficient on APMS(Left : ANN Training, Right : ANN Prediction)

8. Conclusions

Based on the analytical investigation conducted in the course of the current research, it could be concluded that the change in human body's mass, pelvic stiffness, and pelvic damping coefficient give a remarkable change in biodynamic response behaviors of seated human body (direct proportional for human body's mass and pelvic stiffness coefficient and inverse proportional for pelvic damping coefficient.)

Based on the results of implementing the ANN technique in this study, the following can be concluded:

1. The developed ANN models   presented in this study are very successful in simulating the effect of human body's mass and stiffness on the biodynamic response behaviors under whole-body vibration.
2. The presented ANN models are very efficiently capable of predicting the response behaviors at different masses and stiffness rather than those used in the analytic solution.

References

1. Wu X., Rakheja S., and Boileau P.-E., "Analyses of relationships between biodynamic response functions", Journal of Sound and Vibration, Vol. 226, No. 3, PP.595-606, 1999.
2. Coermann R. R., "The mechanical impedance of the human body in sitting and standing position at low frequencies", Human Factors, 227–253, October 1962.
3. Vogt H. L., Coermann R. R., and Fust H. D., "Mechanical impedance of the sitting human under sustained acceleration", Aerospace medicine, Vol. 39, PP. 675-679, 1968.
4. Suggs C.W., Abrams C. F., and Stikeleather L. F., "Application of a damped spring-mass human vibration simulator in vibration testing of vehicle seats", Ergonomics, Vol. 12, PP. 79–90, 1969.
5. Fairley T.E., and Griffin M.J., ''The apparent mass of the seated human body: vertical vibration'' Journal of Biomechanics Vol. 22, No 2, PP. 81–94, 1989.
6. Boileau, P.E., Rakheja, S., Yang X., and Stiharu I.,"Comparison of biodynamic response characteristics of various human body models as applied to seated vehicle drivers", Noise and Vibration Worldwide Vol. 28 ,PP. 7–14, 1997.
7. Toward M.G.R., ''Apparent mass of the seated human body in the vertical direction: effect of holding a steering wheel'', In Proceedings of the 39th United Kingdom Group, Meeting on Human Response to Vibration, Ludlow, 15–17, pp 211–221, 2004.
8. Wang W., Rakhejaa S., and Boileau P.E., "Relationship between measured apparent mass and seat-to-head transmissibility responses of seated occupants exposed to vertical vibration", Journal of Sound and Vibration, Vol. 314, PP. 907-922, 2008.
9. Steina G. J., Mucka P., Hinz B., and Bluthner R., "Measurement and modeling of the y-direction apparent mass of sitting human body–cushioned seat system" Journal of Sound and Vibration, Vol. 322, PP. 454-474, 2009.
10. Tewari V. K., and Prasad N., "Three-DOF modelling of tractor seat-operator system", Journal of Terramechanics, Vol. 36, pp. 207-219, 1999.
11. Boileau, P.E., and Rakheja, S., "Whole-body vertical biodynamic response characteristics of the seated vehicle driver: Measurement and model development", International Journal of Industrial Ergonomics, Vol. 22, pp. 449-472, 1998.
12. Ramanitharan, K. and C. Li, "Forecasting Ocean Waves Using Neural Networks", Proceeding of the Second International Conference on Hydroinformatics, Zurich, Switzerland, 1996.
13. Abdeen, M. A. M., "Neural Network Model for predicting Flow Characteristics in Irregular Open Channel", Scientific Journal, Faculty of Engineering-Alexandria University, 40 (4), pp. 539-546, Alexandria, Egypt, 2001.
14. Allam, B. S. M., "Artificial Intelligence Based Predictions of Precautionary Measures for building adjacent to Tunnel Rout during Tunneling Process" Ph.D., 2005.
15. Azmathullah, H. Md., M. C. Deo, and P. B. Deolalikar, "Neural Networks for Estimation of Scour Downstream of a Ski-Jump Bucket", Journal of Hydrologic Engineering, ASCE, Vol. 131, Issue 10, pp. 898-908, 2005.
16. Abdeen, M. A. M., "Development of Artificial Neural Network Model for Simulating the Flow Behavior in Open Channel Infested by Submerged Aquatic Weeds", Journal of Mechanical Science and Technology, KSME Int. J., Vol. 20, No. 10, Soul, Korea, 2006
17. Abdeen, M. A. M., "Predicting the Impact of Vegetations in Open Channels with Different Distributaries' Operations on Water Surface Profile using Artificial Neural Networks", Journal of Mechanical Science and Technology, KSME Int. J., Vol. 22, pp. 1830-1842, Soul, Korea, 2008.
18. Boileau P.E., "A study of secondary suspensions and human drivers response to whole-body vehicular vibration and shock", PhD. Thesis, Concordia university, Montreal, Quebec, Canada, 1995.
19. Shin, Y., "Neuralyst™ User's Guide", "Neural Network Technology for Microsoft Excel", Cheshire Engineering Corporation Publisher, 1994
20. Mohamed, M. A. M., "Selection of Optimum Lateral Load-Resisting System Using Artificial Neural Networks", M. Sc. Thesis, Faculty of Engineering, Cairo University, Giza, Egypt, 2006.

5/6/2010